Biomaterials Science

Silk Fibroin Gelation via Non-Solvent Induced Phase Separation

Journal:	*Biomaterials Science*
Manuscript ID	BM-ART-10-2015-000471.R1
Article Type:	Paper
Date Submitted by the Author:	09-Dec-2015
Complete List of Authors:	Kasoju, Naresh; Institute of Macromolecular Chemistry, Academy of Sciences of the Czech Republic v.v.i., Biomaterials and Bioanalogous Polymer Systems; University of Oxford, Zoology Hawkins, Nicholas; University of Oxford, Zoology Pop-Georgievski, Ognen; Institute of Macromolecular Chemistry, Academy of Sciences of the Czech Republic v.v.i., Chemistry and Physics of Surfaces and Biointerfaces Kubies, Dana; Institute of Macromolecular Chemistry, Academy of Sciences of the Czech Republic v.v.i., Biomaterials and Bioanalogous Polymer Systems Vollrath, Fritz; University of Oxford, Zoology

Journal Name

ARTICLE

Silk Fibroin Gelation via Non-Solvent Induced Phase Separation†

Naresh Kasoju,[a,b*] Nicholas Hawkins,[b] Ognen Pop-Georgievski,[c] Dana Kubies[a*] and Fritz Vollrath[b*]

Received 00th January 20xx,
Accepted 00th January 20xx

DOI: 10.1039/x0xx00000x

www.rsc.org/

Tissue engineering benefits from novel materials with precisely tunable physical, chemical and mechanical properties over a broad range. Here we report a practical approach to prepare *Bombyx mori* silk fibroin hydrogels using the principle of non-solvent induced phase separation (NIPS). A combination of reconstituted silk fibroin (RSF) and methanol (non-solvent), with a final concentration of 2.5% w/v and 12.5% v/v respectively, kept at 22 °C temperature turned into a hydrogel within 10 hours. Freeze-drying this gel gave a foam with a porosity of 88%, a water uptake capacity of 89% and a swelling index of 8.6. The gelation kinetics and the loss tangent of the gels were investigated by rheometry. The changes in the morphology of the porous foams were visualized by SEM.The changes in RSF chemical composition and the relative fraction of its secondary structural elements were analyzed by ATR-FTIR along with Fourier self-deconvolution. And, the changes in the glass transition temperature, specific heat capacity and the relative fraction of crystallinity of RSF were determined by TM-DSC. Data suggested that RSF – water – methanol behaved as a polymer – solvent – non-solvent ternary phase system, wherein the demixing of the water – methanol phases altered the thermodynamic equilibrium of RSF – water phases and resulted in the desolvation and eventual separation of RSF phase. Systematic analysis revealed that both gelation time and the properties of hydrogels and porous foams could be controlled by the ratios of RSF and non-solvent concentration as well as by the type of non-solvent and incubation temperature. Due to the unique properties we envisage that the herein prepared NIPS induced RSF hydrogels and porous foams can be possibly used for the encapsulation of cells and/or for the controlled release of both hydrophilic and hydrophobic drugs.

1. Introduction

Silk fibers from the cocoons of *Bombyx mori* and other lepidopteran silkworms are composed of two macromolecular protein components viz. sericin and fibroin. The fibroin constitutes about 70-80% of total cocoon weight and forms the filamentous core. *Bombyx* fibroin filaments contain a 'heavy' protein chain of approximately 350 kDa, a 'light' chain of around 25 kDa and a P25 protein of about 27 kDa with altogether high percentages of glycine, alanine and serine.[1] The sericin, 'gum' protein that glues the fibrous filaments together, contributes about 20-30% of total cocoon weight; on the other hand has high percentages of threonine and tyrosine as well as serine.[2] Because of their biodegradability and biocompatibility, natural silks have long been used as resorbable surgical sutures, and more recently their use has expanded into tissue engineering and allied fields.[3] Major biomaterial assets of fibroin are: i) excellent compatibility with mammalian cells including somatic, blood and stem cells, ii) versatile reactivity in aqueous or organic solvents, iii) bulk and surface level modification/ functionalization options and iv) the ability to tune the mechanical and degradation properties of filaments and threads.[4]

Several kinds and classes of silk fibroin based materials were developed for potential applications in tissue engineering, regenerative medicine, artificial disease tissue model development and controlled therapeutic release. Specific examples would be woven or nonwoven networks made of native fibers, and porous foams, films/ membranes, hydrogels and micro- or nano- particles created from the reconstituted aqueous solution of fibroin.[3-5] Solubility in solvents other than water enable the fabrication of submicron- or nano- fibrous matrices by electrospinning.[6] However, more than any other forms of materials, the hydrogels and the porous foams are regarded as the ideal classes of materials, for selected biomedical applications, since their interconnected porous network with high water content resemble the natural soft tissue matrix.[7] In particular, the silk fibroin hydrogels and porous foams are of special interest as the block copolymer nature can be explored to control the secondary structure and crystallinity of the protein. By this, we can eventually tune the stiffness of the matrix to modulate the cell response and/or to control the drug release kinetics. Additionally, besides the encapsulation of hydrophilic therapeutic molecules, the hydrophobic pockets of fibroin can be exploited for the encapsulation of hydrophobic drug molecules.

[a] Department of Biomaterials and Bioanalogous Polymer Systems, Institute of Macromolecular Chemistry, Academy of Sciences of the Czech Republic, v.v.i., Prague, Czech Republic. Email: kasoju@imc.cas.cz (NK), kubies@imc.cas.cz (DK)
[b] Department of Zoology, University of Oxford, Oxford, United Kingdom. Email: fritz.vollrath@zoo.ox.ac.uk (FV)
[c] Department of Chemistry and Physics of Surfaces and Biointerfaces, Institute of Macromolecular Chemistry, Academy of Sciences of the Czech Republic, v.v.i., Prague, Czech Republic.
† Electronic Supplementary Information (ESI) available: See DOI: 10.1039/x0xx00000x

Traditionally, we can dissolve the silk fibroin fibers and prepare an aqueous reconstituted silk fibroin (RSF) solution. However, with 79% of hydrophobic residues, the fibroin exist in a meta-stable state which is highly vulnerable to any factor that can drive the self-assembly of less-ordered randomly coiled fibroin molecules into ordered crystalline β-sheet aggregates.[8, 9] Previously, a variety of physical and chemical stimuli were exploited to produce RSF hydrogels. For example, RSF gelation was demonstrated by lowering the pH of RSF solution close to its isoelectric point (4.8 to 5.0)[10], by exposing to CO_2 under high pressure[11], by applying shear stress either by vortexing[12] or by sonication[13]. While the preparation of RSF porous foams were demonstrated by simply freeze-drying the RSF solution and exposing it to methanol to make water-stable. However, the fabrication of foams by freeze-drying the hydrogels is an interesting approach since they allow the encapsulation of cells and drugs.[14] But, the pH or CO_2 induced gelation protocols do not allow the encapsulation of cells or other pH sensitive therapeutic molecules. The vortex or sonication induced methods do support such encapsulation, but, in our personal experience we found that some amount of RSF was precipitated during processing and the amount of such precipitate was changing from batch to batch; this inconsistency in the RSF content can affect the final gel properties. Moreover, all of these methods, at least in our knowledge, were based on aqueous RSF solutions, therefore they only allow the encapsulation of cells and hydrophilic drugs but not hydrophobic drugs.

In order to prepare the hydrogels that can be used for the encapsulation of cells and/or hydrophilic and hydrophobic drug molecules, here we investigated the use of an organic solvent, i.e. a non-solvent for RSF, as the gelation inducer by following the principle of non-solvent induced phase separation (NIPS). Subsequent freeze-drying could yield the porous foams which do not require further cross-linking or other processing steps. We propose that the addition of polar protic organic solvents such as methanol, ethanol, iso-propanol and n-butanol to the fibroin – water mixture disturbs the hydrophobic hydration of RSF, causes the desolvation of RSF and leads to the self-assembling of RSF. Our hypothesis is based on the use of methanol as a cross-linking or β-sheet inducing agent in the post-processing of RSF based biomaterial scaffolds. For example, the stability of the fibroin – gelatin films prepared by spin coating and fibroin – galactosylated chitosan nanofibrous scaffolds prepared by electrospinning were improved by a post-fabrication methanol treatment.[6, 15] Addition of methanol during processing was also effective in producing high crystalline RSF powders or porous foams.[16, 17] Thus, here we studied the use of methanol to induce the conformational transition of RSF and its effects on RSF aggregation/ gelation. We performed systematic investigations to determine the effects of organic solvent content, fibroin concentration, as well as organic solvent type and incubation temperature on the gelation time and gel properties by tracking gelation kinetics, morphology and secondary structure by rheology, SEM, ATR-FTIR and TM-DSC.

2. Materials and methods

2.1 Materials

We purchased *Bombyx mori* cocoons from Padua Silk Station in Italy, the chemicals sodium carbonate, lithium bromide, methanol, ethanol and dimethyl sulfoxide from Sigma-Aldrich, UK, isopropanol from VWR International Ltd, UK, n-butanol from Fisher Scientific, UK, dialysis tubing (WMCO 12-14 kDa) from Visking, UK, and n-hexane from Lach-ner s.r.o., Czech Republic.

2.2 Preparation of reconstituted silk fibroin (RSF)

B. mori cocoons were degummed and processed to yield aqueous RSF solution by following the conventional method (**Figure 1**).[5] Briefly, 10 g of cocoons were cut into small pieces and degummed in 4 L (2 × 2 L) of boiling 0.1% sodium carbonate solution for 30 min. The fibers were thoroughly washed with ultrapure water and air-dried. The degummed fibers were then dissolved in 9.3 M lithium bromide, in the ratio of 1 g : 4 mL, at 60 °C for 4 h. The resulting solution was carefully poured into a dialysis bag and dialyzed against ultrapure water for 48 h, with intermittent water exchange for 6 times. Once dialyzed, the aqueous RSF solution was centrifuged to remove the insoluble matter, collected in a clean vial and stored at 4 °C until further use.

To determine the concentration of RSF in the solution, the weight of a small weigh boat was measured, 0.5 ml of RSF solution was added to the boat and it was then air-dried in a hood. Once the solution was dried, the weight of the boat was measured again. The difference between the final and the initial weights of boat was the weight of RSF; and dividing this by 0.5 ml yielded RSF concentration in the weight per volume percentage. The final RSF concentration was found to be little higher than 10% (w/v); therefore, when required, the original solution was diluted with ultrapure water to prepare the solutions with a lower RSF concentration.

2.3 Fabrication of hydrogels and porous foams

The process of hydrogel and foam preparation was simple and straightforward (**Figure 1**). In an experiment, RSF solution (typically with a working concentration of 5% w/v in water) and an organic solvent (typically methanol with a working concentration of 25% v/v in water) were mixed in 1:1 (v/v) ratio. This gives a solution with a final RSF concentration of 2.5% w/v and a methanol content of 12.5% v/v. The solution was vortexed at 1500 rpm for 3 min and at 2000 rpm for another 1 min, and then incubated typically at ambient temperature (22 °C). The solutions were manually inspected at regular intervals to check the gelation. Once the gel was formed, it was collected in a fresh vial and gently washed with ultrapure water to remove the residual organic solvent. Initially the gel floats in the water, but it settles down once the organic solvent was washed out (**Figure S1**). For making the porous foams, the gels were frozen in -20 °C freezer for 6 hours and were then subjected to lyophilization at -45 °C temperature and 90 mTor vacuum for 1 day. The details of the parameters under study are described in the **Table 1**.

Table 1. Details of various parameters studied along with the variable and constant conditions followed. In all cases the total volume of the reaction mixture was kept constant.

Parameter	Variables	Constants
Methanol (non-solvent) content	0, 5, 12.5, 25, 37.5 and 50% (v/v)	[RSF] = 2.5% (w/v), temperature = 22 °C
RSF concentration	1.25, 2.5, 3.75 and 5% (w/v)	[Methanol] = 12.5% (v/v), temperature = 22 °C
Incubation temperature	4, 22 and 37 °C	[RSF] = 2.5% (w/v), [Methanol] = 12.5% (v/v)
Non-solvent type	Methanol, ethanol, isopropanol, n-butanol and DMSO	[RSF] = 2.5% (w/v), [Non-solvent] = 12.5% (v/v), temperature = 22 °C

Figure 1. Schematic of the NIPS induced RSF hydrogels and porous foams preparation: *B. mori* cocoons were first degummed in the boiling sodium carbonate solution to yield the pure fibroin fibers. The fibers were dissolved in the lithium bromide solution and the mixture was dialyzed against water to yield the aqueous solution of reconstituted silk fibroin or RSF. RSF solution was mixed with a definite amount of methanol and subjected to mild vortexing and then incubated at a preset temperature to become hydrogels. The hydrogels were collected and rinsed with water to washout the traces of methanol. Alternatively, the hydrogels may be subjected to freeze-drying to yield the porous foams.

2.4 Characterization methods

2.4.1 Gelation time. The vials with the solutions were tilted at 45° angle at regular intervals in order to determine the physical state. The solution was considered to have gelled when the meniscus did not deform upon tilting at 90° angle. In addition, the self-supporting state of gels was checked by turning the tubes upside down. The time to reach such gelled state was defined as the critical time for gelation. The effects of organic solvent content, RSF concentration, incubation temperature and type of organic solvent used on the time of gelation were systematically studied as shown in **Table 1**.

2.4.2 Porosity. The porosity of the porous foams (freeze-dried hydrogels) was measured by the conventional liquid displacement method.[18] A sample of the weight W was immersed in a known volume (V_1) of hexane in a graduated cylinder for 5 min. The total volume of hexane and the hexane-saturated scaffold was recorded as V_2. The scaffold was removed and the residual hexane volume was recorded as V_3. The volume difference of $V_2 - V_1$ was the volume of the scaffold. The volume of hexane within the scaffold ($V_1 - V_3$) was determined as the void volume of the scaffold. The cumulative volume of the scaffold was $V_2 - V_3$. The percentage of porosity was obtained from the equation (1).[18] The porosities of the freeze-dried gels prepared with varying organic solvent content, RSF concentration, incubation temperature and type of organic solvent were systematically studied (**Table 1**).

$$\text{Porosity (\%)} = \frac{V_1 - V_3}{V_2 - V_3} \times 100 \qquad \text{Equation (1)}$$

2.4.3 Swelling index and water uptake capacity. To study the swelling index and the water uptake capacity, the porous foams (freeze-dried hydrogels) of pre-determined weight (W_d, dry weight) were immersed in the ultrapure water for 24 h at 37 °C. The swollen foams were gently rolled-over a clean tissue paper to remove the excess water, and then, their wet weight (W_s, swollen weight) was noted immediately. The swelling index was calculated from the equation (2),[19] while the water uptake capacity was calculated from the equation (3).[20] The swelling and water uptake properties of the freeze-dried gels prepared with varying organic solvent content, RSF concentration, incubation temperature and type of organic solvent were systematically studied (refer to **Table 1** for details).

$$\text{Swelling index} = \frac{W_s - W_d}{W_d} \qquad \text{Equation (2)}$$

$$\text{Water uptake (\%)} = \frac{W_s - W_d}{W_s} \times 100 \qquad \text{Equation (3)}$$

2.4.4 Scanning electron microscopy (SEM). The morphology of the porous foams (freeze-dried hydrogels) prepared with varying organic solvent concentration, RSF

concentration, incubation temperature and type of organic solvent (refer to **Table 1** for details) was examined using a table top SEM (Neoscope JCM-5000, JEOL). For this purpose, the samples were mounted on the specimen holder with an electro-conductive tape, sputter-coated with Platinum under argon gas in a coating unit (SC7620, Polaron range), and subsequently analyzed by SEM.

2.4.5 Rheometry. To understand the typical aggregation/ gelation kinetics, a solution of RSF (with a final concentration of 2.5% w/v) mixed with methanol (with a final content of 12.5% v/v) was vortexed at 1500 rpm for 3 min, then at 2000 rpm for another 1 min, and was immediately studied for its storage (elastic, G') and loss (viscous, G'') moduli as functions of time (for a period of 20 h) at 1 Hz frequency, 5% strain and 25 °C temperature.

To study the effects of the organic solvent content on the rheological properties, a solution of RSF (a final concentration of 2.5% w/v) mixed with a variable amount of methanol (a final content of 5, 12.5, 25, 37.5 and 50% v/v) was vortexed at 1500 rpm for 3 min, then at 2000 rpm for another 1 min, and was immediately studied for its storage (G') and loss (G'') moduli as functions of frequency (ranging from 0.1 to 10 Hz) at 5% strain and 25 °C temperature. The measurement of 2.5% w/v RSF mixed with 50% v/v or higher content of methanol was not possible as it was gelled prior to the loading onto the rheometer.

All the rheological measurements were performed on a high resolution rheometer (CVO 120, Bohlin) using the cone-plate geometry, with a 40 mm cone diameter, 4° angle, and 150 µm gap. During the measurement, the temperature of the sample holder was maintained at 25.0 ± 0.1 °C, and a humid solvent trap was employed around the sample holder to confront the organic solvent evaporation. For comparison purpose, RSF solution (a final concentration of 2.5% w/v) without any methanol was considered as the control.

2.4.6 Attenuated total reflection Fourier transform infra-red (ATR-FTIR) spectroscopy. The porous foams (freeze-dried hydrogels) prepared from RSF (with a final concentration of 2.5% RSF w/v) mixed with varying amounts of methanol (with a final content of 0, 5, 12.5, 25, 37.5 and 50% v/v) were analyzed by an FTIR spectrometer (6700, Thermo Nicolet), equipped with an ATR attachment (Golden Gate, Specac). During the measurements, the instrument was continuously purged by nitrogen using blow-off from a liquid nitrogen tank to eliminate the spectral contributions of atmospheric water vapor. For each measurement, 64 scans were recorded with a resolution of 2 cm^{-1} and the wavenumbers ranging from 500 to 6000 cm^{-1}. The signature spectra of amide-I region between 1600 to 1700 cm^{-1} were baseline corrected and were resolved by the Fourier self-deconvolution (FSD) approach using the Nicolet OMNIC and the Origin software. FSD was performed in accordance with previously described procedures using the following parameters: a half-bandwidth (full-width at half-height) of 25 cm^{-1}, enhancement factor (*K* value) of 2.7 and Gaussian profiles to fit the resulting FSD envelope. [21-23]

The fitting procedure proceeded as follows: a) The initial band positions were fixed at 1595 cm^{-1} (side chains), 1610 cm^{-1} (side chains), 1620 cm^{-1} (intermolecular β-sheets), 1630 cm^{-1} (intermolecular β-sheets), 1640 cm^{-1} (random coils), 1650 cm^{-1} (random coils), 1660 cm^{-1} (α helices), 1670 cm^{-1} (β-turns), 1680 cm^{-1} (β-turns), 1690 cm^{-1} (β-turns) and 1700 cm^{-1} (intramolecular β-sheets), allowing for the height and width of the bands to vary; b) In the second step, the position of the bands was allowed to vary in the range of ±5 cm^{-1} from the initial seeding value using the Levenberg-Marquardt algorithm; c) Finally, a nonlinear least-squares method was used to fit the reconstituted curve as close as possible to the FSD spectra.

2.4.7 Temperature modulated differential scanning calorimetry (TM-DSC). The TM-DSC measurements of the porous foams (freeze-dried hydrogels) prepared from RSF (with a final concentration of 2.5% RSF w/v) mixed with varying amounts of methanol (i.e., with a final content of 0, 5, 12.5, 25, 37.5 and 50% v/v) were recorded using a DSC instrument equipped with a refrigerated cooling system (Q2000, TA Instruments). Approximately 5 mg of a sample was carefully encapsulated in an aluminum (Al) pan with the special sample preparation accessory supplied with the instrument. The lid of the pan was carefully punctured to avoid the pressurization and bursting during the measurements. The thermograph was obtained from 10 to 235 °C temperature with a heating rate of 2 °C/min, modulation period of 60 s and temperature amplitude of 0.318 °C. Before each run, the samples were thoroughly dried under vacuum at ambient temperature to eliminate the surface water absorbed during handling. During the measurements, the cell was purged with dry nitrogen at a rate of 20 cc/min. The instrument was calibrated with an empty cell for the baseline correction, and with indium filled cell for the heat flow and temperature correction.

The total heat flow, reversing heat flow and specific heat capacity of the samples were calculated by using the software supplied with the instrument and Origin software and by following an earlier report of Hu et al., 2006.[21] The fraction of mobile (ϕ_{Mobile}, less-ordered non-crystalline mobile component) and rigid (ϕ_{Rigid}, ordered crystalline + semi-crystalline immobile components) secondary structures were calculated using equation (4), where, ΔC_p^{sc} and ΔC_p^{nc} indicate changes in the specific heat capacities of the semi-crystalline and the non-crystalline samples respectively.[21]

$$\phi_{\text{Mobile}} = \Delta C_p^{sc} / \Delta C_p^{nc} \qquad \text{Equation (4a)}$$

$$\phi_{\text{Rigid}} = 1 - \phi_{\text{Mobile}} \qquad \text{Equation (4b)}$$

3. Results and discussion

3.1 Effect of non-solvent (methanol) content

The effect of methanol content on RSF gelation were studied by changing methanol content from 0 to 5, 12.5, 25, 37.5 and 50% (v/v) (**Table 1**). The final RSF concentration was at 2.5% (w/v) and the temperature was 22 °C. Within an overnight incubation study, RSF solution with 5% v/v of methanol

remained clear, while the solutions containing 12.5% v/v or above of methanol got gelled (**Figure 2a**). The time of gelation was 10 h when methanol content was 12.5%, but, it decreased to a mere 25 s when methanol was changed to 50% (**Table 2**). Since RSF concentration and the total volume of the solution were kept constant, it was therefore evident that the addition of non-solvent did indeed caused the conformational changes in RSF that eventually led to its aggregation and subsequent gelation, and we proved this in the subsequent rheology, FTIR and DSC analysis. Further, the rate of gelation was directly correlated with the amount of non-solvent. Both observations agree with previous reports where ethanol was used as a non-solvent to prepare RSF based micro/submicron scale particles and where the amount of ethanol decreased the size but increased the total yield of particles (because, with a lower ethanol content, the nucleation was slower, the total number of nucleation points was lower and with time the nucleates grew and increase in size; while with a higher ethanol content, the nucleation was faster, the total number of nucleation points was higher but there was no scope for nucleate growth and therefore they remained smaller in size).[24, 25]

Table 2. Gelation time and other physical properties of the gels prepared by varying methanol (non-solvent) content, RSF concentration, incubation temperature and type of non-solvent.

Parameter		Gelation time	Porosity (%)[†,#]	Swelling index[†,##]	Water uptake (%)[†,##]
Methanol (non-solvent) content (%, v/v)	0	N[*]	90.7 ± 0.4	N[**]	N[**]
	5	N[*]	88.9 ± 0.5	9.0 ± 0.4	90.0 ± 0.4
	12.5	10 ± 0.75 h	88.2 ± 0.6	8.6 ± 0.2	89.5 ± 0.2
	25	25 ± 5 min	86.8 ± 0.8	8.1 ± 0.4	89.0 ± 0.5
	37.5	3 ± 0.5 min	66.2 ± 4.7	1.6 ± 0.1	60.8 ± 0.5
	50	25 ± 5 sec	60.8 ± 7.9	1.2 ± 0.1	55.3 ± 0.6
RSF concentration (%, w/v)	1.25	11 ± 0.75 h	89.5 ± 0.4	9.4 ± 0.3	90.4 ± 0.3
	2.5	10 ± 0.75 h	88.2 ± 0.6	8.6 ± 0.2	89.5 ± 0.2
	3.75	9.5 ± 0.5 h	87.3 ± 0.4	7.8 ± 0.2	88.7 ± 0.3
	5	9 ± 0.5 h	85.2 ± 0.6	7.0 ± 0.1	87.4 ± 0.2
Incubation temperature (°C)	4	6 ± 0.5 h	86.2 ± 0.5	8.1 ± 0.4	89.0 ± 0.4
	22	10 ± 0.75 h	88.2 ± 0.6	8.6 ± 0.2	89.5 ± 0.2
	37	11 ± 0.75 h	88.7 ± 0.3	8.7 ± 0.3	89.7 ± 0.3
Non-solvent type	Methanol	10 ± 0.75 h	88.2 ± 0.6	8.6 ± 0.2	89.5 ± 0.2
	Ethanol	10 ± 0.5 h	88.0 ± 0.7	8.4 ± 0.3	89.3 ± 0.3
	Isopropanol	9.5 ± 0.5 h	86.4 ± 1.2	8.1 ± 0.4	89.0 ± 0.4
	n-Butanol	4 ± 0.5 h	85.7 ± 0.8	7.7 ± 0.3	88.5 ± 0.4
	DMSO	N[*]	74.8 ± 2.6	5.4 ± 0.2	84.4 ± 0.5

[*]No gelation was observed within an overnight incubation. [**]Measurement not possible since the foam collapsed and partially dissolved in water. [†]Properties of freeze-dried form of hydrogels. [#]Medium was hexane. [##]Medium was ultrapure water.

The physical observation of the porous foams (freeze-dried hydrogels) revealed significant size shrinkage with a stiffer and harder structure at and above 25% of methanol content (**Figure 2b**). The effects of methanol fraction were also evident at the microscopic level. As shown by SEM imagery (**Figure 2i-2vi**), the sheet-like or micro-tubular porous structure with the high porosity typical for the control samples (no methanol added) was transformed into the densely packed randomly porous structure with reduced porosity upon gradual increase in methanol content to 50%. The morphological observations were consistent with the porosity which was found to decrease from 88 to 60% when methanol content increased from 12.5 to 50% (**Table 2**). And, as anticipated, the water uptake capacity and the swelling index showed a similar decrease from 90% to 55% and from 8.6 to 1.2, respectively, when methanol content was changed from 12.5 to 50% (**Table 2**). The transformation in the morphology and reduction in the porosity and other physical properties of RSF freeze-dried hydrogels prepared by NIPS in the current study are in a good agreement with the earlier reports on RSF porous scaffolds prepared by TIPS (thermally induced phase separation).[16, 17, 26]

3.2 Effect of RSF concentration

The effect of RSF concentration on the gelation were studied by changing the final RSF concentration viz. 1.25, 2.50, 3.75 and 5.00% w/v with methanol content constant at 12.50% v/v (**Table 1**). Within an overnight incubation study, the gelation was achieved at all the tested RSF concentrations (**Figure 3a**). The time of gelation decreased from 11 h to 9 h when RSF concentration increased from 1.25 to 5.00 % (**Table 2**). The increase in the polymer concentration increases the crowding of the polymer molecules and alters the relative volume fraction of the polymer to the solvent. For example, considering methanol content as constant at 12.50%, a 1.25% RSF solution contains a water fraction of 86.25%, while a 5% RSF solution contains a reduced water fraction of 82.50 % only. Such a crowding of RSF molecules along with the changes in the relative ratio of water – methanol lead to enhanced interactions amongst them and eventually resulted in rapid aggregation. These observations were very similar to the effects of RSF concentration on RSF gelation, induced in presence of a constant amount of Ca^{2+} (5 mM) and poly(ethylene oxide) (5% w/v) in the solution.[27]

As presented in **Figure 3b**, the porous foams (freeze-dried hydrogels) showed no noticeable size shrinkage at the

macroscopic level. However, as evident from the SEM images (**Figure 3i-3iv**), the effects of RSF content are obvious at the microscopic level. It appeared that the pore size gradually decreased with increased RSF concentration. And, as calculated by the liquid displacement method, the porosity decreased from 90% to 85% respectively when the RSF concentration increased from 1.25 to 5% (**Table 2**). As reported previously for porous polymer foams prepared by TIPS, the pores were generated by the separation and subsequent removal of the polymer-lean (or solvent) phase. Any change in the relative content of the polymer-rich and polymer-lean phases greatly affected the pore properties, i.e., the increasing polymer content led to the reduced solvent content thus reduced pore structure and vice versa.[26, 28] We also observed a slight decrease in the water uptake capacity from 90 to 87% and in the swelling index from 9.4 to 7.0 when RSF concentration increased from 1.25 to 5.00% (**Table 2**). However, we found that the changes in the gelation times and other properties observed here were not as much as they were with increasing methanol content; this suggested the critical role of methanol as the sole inducer of the RSF gelation.

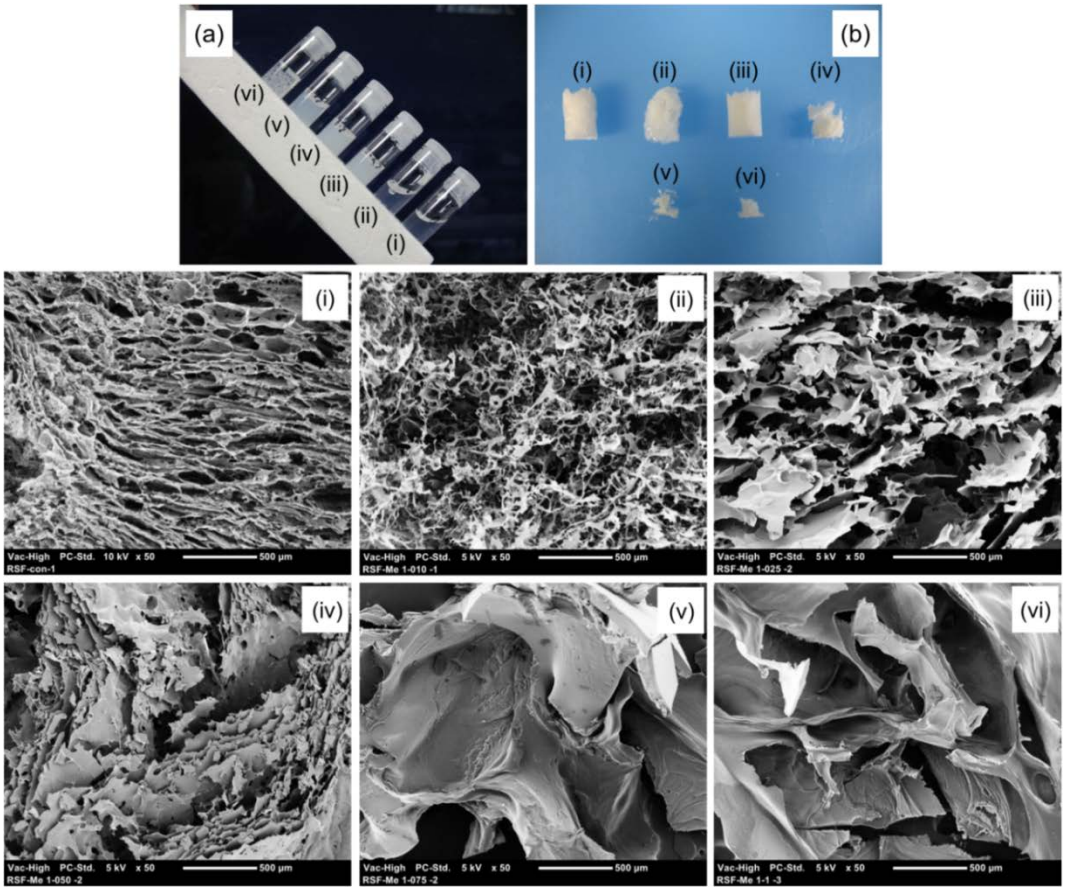

Figure 2. Effect of methanol content: Visual inspection (a) of hydrogels prepared from 2.5% RSF mixed with 0 (i), 5 (ii), 12.5 (iii), 25 (iv), 37.5 (v) and 50% v/v (vi) of methanol showed the gelation in the samples with 12.5% or a higher methanol content only. (b) The porous foams (freeze-dried hydrogels) showed a size reduction in the samples with 25% or higher methanol content. The SEM images of the porous foams revealed the sheet-like or micro-tubular porous structure in the control sample (i), fibrous nature in the sample with low methanol (ii), a good porous structure in the sample with 12.5% methanol (iii), and the less-porous or collapsed structure in the samples with 25% or higher methanol (iv-vi).

3.3 Effect of temperature

To investigate the effect of the incubation temperature on the gelation, we prepared the samples with a constant content of RSF (2.5% (w/v) and methanol (12.5% (v/v) at 4, 22 and 37 °C temperature (**Table 1**). Gelation was achieved at all the temperatures tested within an overnight incubation study (**Figure 4a**) and the gelation time increased from 6 to 11hrs when the temperature increased from 4 to 37 °C (**Table 2**). The observed direct correlation between temperature and gelation time contradicts the previous reports, which showed an inverse correlation.[27, 29] RSF solutions in the earlier reports were without any additives; in contrast, here RSF solution was mixed with methanol. It was possible that methanol may have evaporated partly from the reaction mixture at 37 °C; but this may not be the case at 4 °C. Therefore, methanol content in the solution incubated at 37 °C was relatively lower and thus led to delayed gelation, while methanol content in the solution incubated at 4 °C was higher and thus led to quicker gelation. This observation further confirms the role of methanol as the sole inducing factor for RSF gelation.

The physical observation of the porous foams (freeze-dried hydrogels) revealed no noticeable size shrinkage at the macroscopic level (**Figure 4b**). However, the SEM images

revealed the apparent effects of temperature at the microscopic level (**Figure 4i-4iii**). The images suggested a gradual decrease in the pore size with an increase in the incubation temperature. It appeared that the silk fibroin molecules in presence of methanol and at higher temperature were prone to stronger physical cross-linking that gradually led to a coalesced polymer-rich phase; this consequently led a decrease in the pore size with increased temperature. These morphological observations correlate with the earlier reports which showed a thicker polymer-rich phase and a decrease in the pore size with an increase in the gelation temperature.[27, 29] Further, the porosity slightly increased from 86 to 89% when the temperature increased from 4 to 37 °C, but no significant changes were observed in the water uptake capacity and the swelling index (**Table 2**).

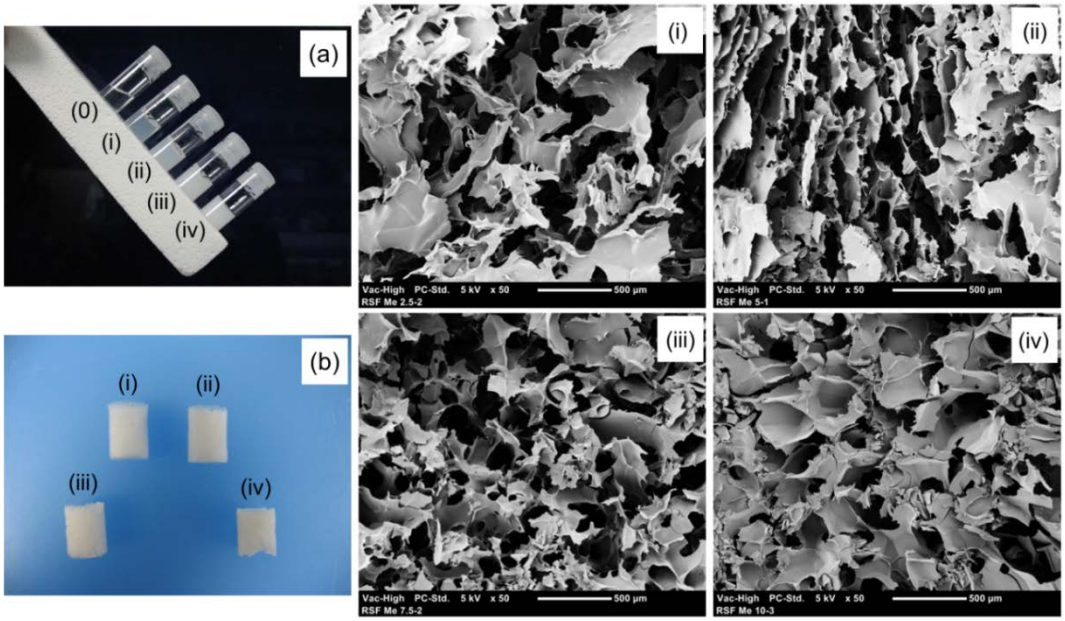

Figure 3. Effect of RSF concentration: Visual inspection (a) of hydrogels prepared from 1.25 (i), 2.5 (ii), 3.75 (iii) and 5% w/v (iv) of RSF mixed with 12.5% v/v methanol showed the gelation in all the samples. (b) The porous foams (freeze-dried hydrogels) showed no significant size reduction. The SEM images of the porous foams revealed a good porous structure in all the samples and a reduction in the pore size with an increasing RSF concentration. (a0: 2.5% w/v RSF without methanol)

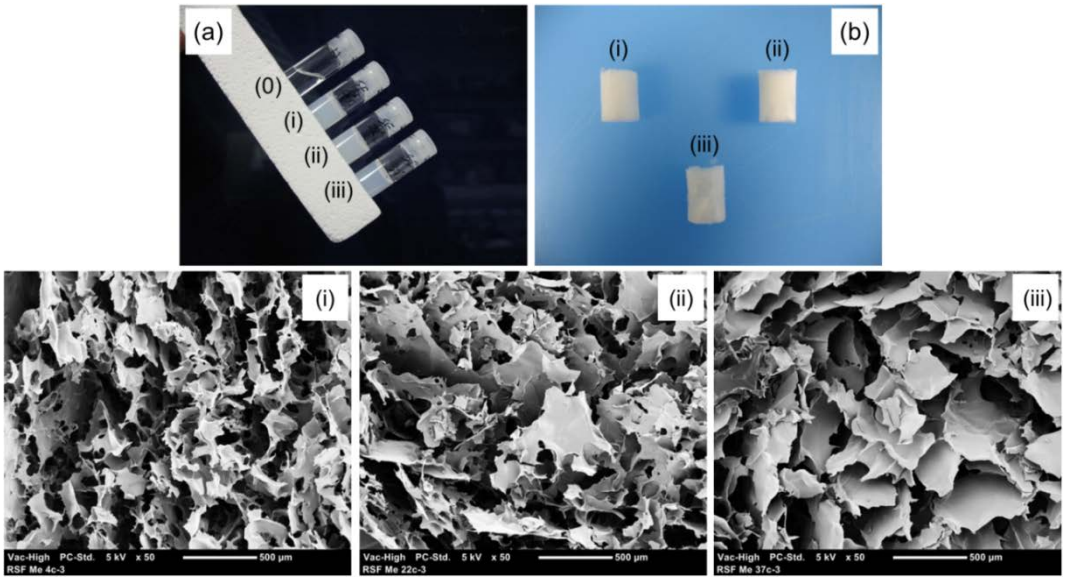

Figure 4. Effect of gelation temperature: Visual inspection (a) of hydrogels prepared from 2.5% w/v RSF and 12.5% v/v methanol at 4 (i), 22 (ii) and 37 °C (iii) temperature showed the gelation in all the samples. (b) The porous foams (freeze-dried hydrogels) showed no significant size reduction. The SEM images of the porous foams revealed a good porous structure in all the samples and a reduction in the pore size with an increasing gelation temperature. (a0: 2.5% w/v RSF without methanol)

3.4 Effect of non-solvent type

To determine the versatility of the non-solvent induced phase separation of RSF, we investigated the possibility of gelation by other similar organic solvents such as ethanol, isopropanol, n-butanol and DMSO. For this purpose, the samples containing a constant final RSF content of 2.5% (w/v) and a constant final amount of organic solvent of 12.5% (v/v) were prepared at 22 °C temperature (**Table 1**). Within an overnight incubation study, the gelation was achieved with all the tested alcohols (**Figure 5a**). Methanol, ethanol and isopropanol induced RSF gelation in 10 h with a little relative time difference, but, n-butanol led to RSF gelation in just 4 h (**Table 2**). Generally, the polarity of the alcohols or their solubility in water is determined by the relative strength of the polar OH group vs the nonpolar carbon chain. Due to the stronger OH group, methanol, ethanol and isopropanol behave as polar solvents and are completely water miscible. But, n-butanol with its 4-carbon chain behaves as a nonpolar solvent with relatively lower water miscibility.[30] And, RSF with its 79% of hydrophobic residues exists in a metastable state.[8] It was possible that in comparison to the low carbon chain alcohols, the stronger repulsive forces exerted by n-butanol forced RSF to self-assemble into hydrogels relatively quicker.

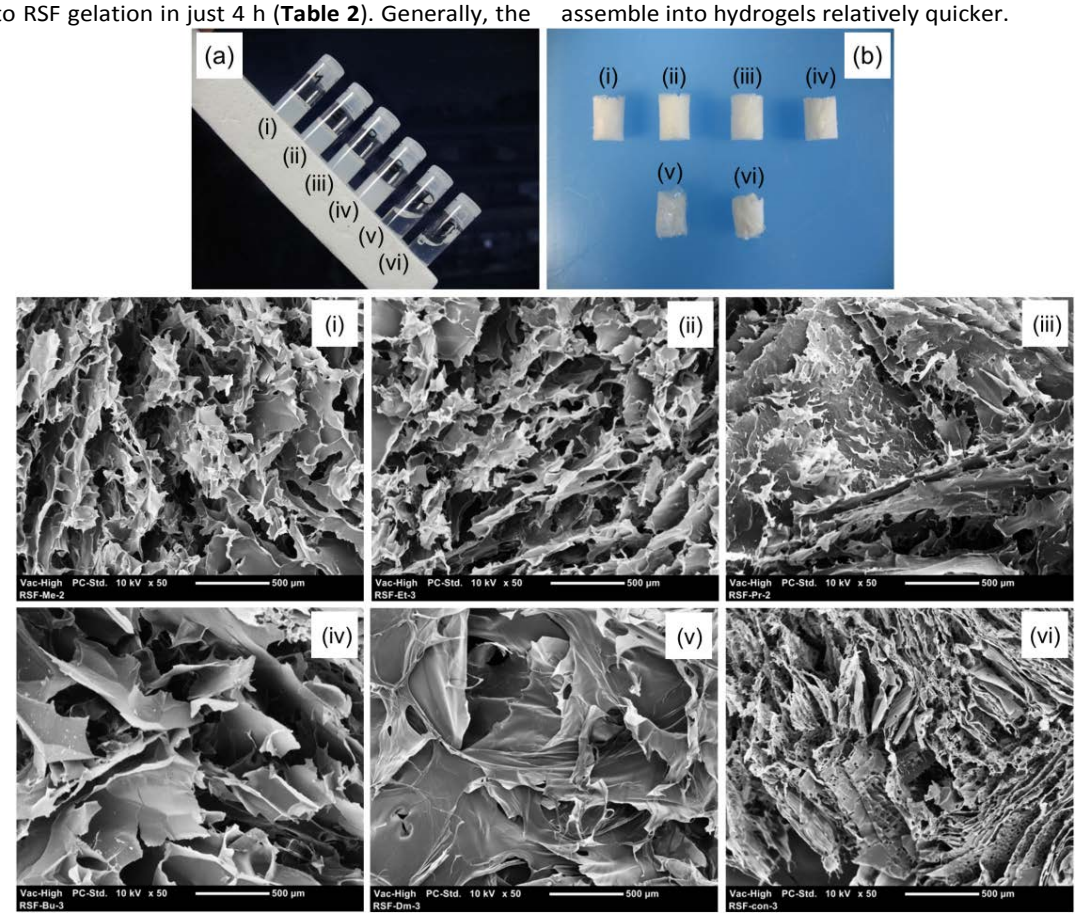

Figure 5. Effect of solvent type: Visual inspection (a) of hydrogels prepared from 2.5% w/v RSF and 12.5% v/v of methanol (i), ethanol (ii), isopropanol (iii), n-butanol (iv), dimethyl sulfoxide (v) and water (vi), showed the gelation in the samples with protic organic solvents only. (b) The porous foams showed no significant size reduction. The SEM images of the porous foams revealed a reduction in the pore size when the non-solvent was changed from methanol to n-butanol.

The size shrinkage of the porous foams (freeze-dried hydrogels) was not noticeable (**Figure 5b**). However, the SEM analysis revealed that the pore size gradually decreased with increased carbon chain length of alcohols (**Figure 5i-5vi**). With porosity, the water uptake capacity and swelling index slightly decreased from 88 to 86%, 90 to 89% and 8.6 to 7.7, respectively, when the solvent was changed from methanol to butanol (**Table 2**). In contrast to the protic alcohols, the gelation was not achieved with DMSO, at least during the overnight incubation at room temperature (**Figure 5a**, vial v). The aprotic nature of DMSO may be attributed for its inability to induce the intermolecular hydrogen bonding in RSF unlike the protic alcohols.[26] Nevertheless, the solution when freeze-dried yielded porous foams.[26, 31] In comparison to the foams created with alcohols, the foams made with DMSO showed significant volume shrinkage, reduced pore size, porosity of 75%, water uptake capacity of 85% and swelling index of 5% (sample v of **Figure 5**, and **Table 2**).

3.5 Insights into gelation kinetics and behavior from rheometry

To understand the typical gelation kinetics of RSF in presence of a non-solvent, we investigated the elastic storage modulus (G′) and viscous loss modulus (G″) of RSF (2.5% w/v) without (control) and with methanol (12.5% v/v, test) as a function of time. As presented in the **Figure 6a**, in the test sample, both G′ (0.02 Pa) and G″ (0.07 Pa) were very low at the beginning of the analysis. The tan δ of >1 indicated the sol-like behavior of the sample. As the time proceeded, there was a crossover of G′ and G″ with a tan δ = 1 at 8.7 h. The crossover was defined

as the gel point. Thereafter both moduli elevated rapidly with time. After 13 hrs, both moduli stabilized and remained largely unaltered (G' of 5.0 × 10^3 Pa and G" 0.25 × 10^3 Pa) for the rest of measurement time and the tan δ of <1 indicated the gel-like behavior of the sample. In contrary, both moduli remained unchanged for the entire measurement time in case of the control sample, with no distinct gelation point and with a tan δ of >1 that represent the sol-like behavior of the sample. The kinetics of the non-solvent induced RSF gelation in the current report matches with those of RSF gelation induced by changing pH,[10] applying electric field,[32] or by blending with hydroxypropylcellulose,[33] Poly(N-isopropylacrylamide).[34] However, the gelation time was not comparable as the solution properties such as RSF concentration and the measurements parameters such as frequency, strain and temperature influenced the rate of gelation.

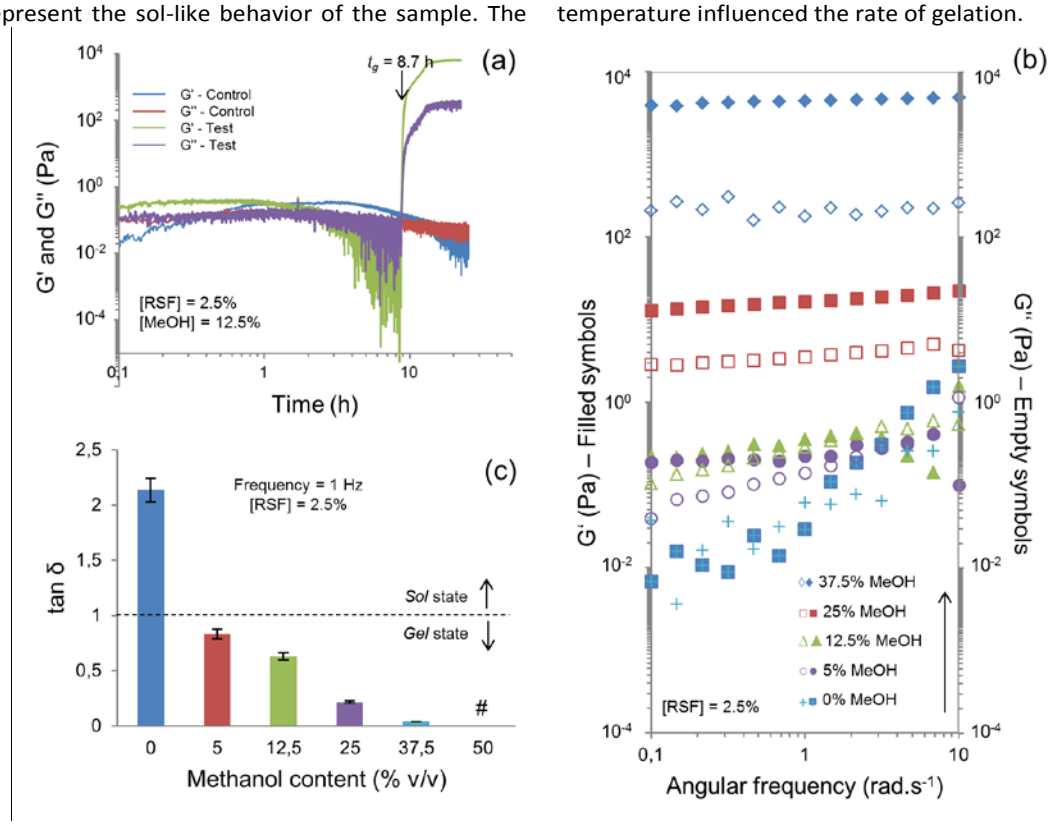

Figure 6. Rheological measurements: (a) The time sweep studies of RSF mixed with methanol (test) revealed the gelation point (t_g) or the crossover of storage (G') and loss (G'') moduli at 8.7 h, while RSF mixed with water (control) showed no such behavior. The noise before the gelation point may be caused by the conformational changes occurring in the fibroin and/or by other technical factor(s). (b, c) The frequency sweep studies of RSF mixed with increasing amount of methanol showed an increase in the moduli and a decrease in the loss tangent (tan δ, data expressed as mean ± standard error) and thus suggested an increase in the gel strength. #Measurements of RSF mixed with 50% methanol were not possible since the gelation occurred before loading to the rheometer.

To determine the effects of methanol content on the rheological properties of gels, we investigated the storage (G') and loss (G") moduli of RSF (2.5% w/v) with various methanol contents (0, 5, 12.5, 25 and 37.5% v/v) as a function of frequency. As shown in **Figure 6b** and **6c**, the measurements revealed three compelling observations. Firstly, at 1 Hz frequency, RSF without methanol showed a tan δ >1, while RSF mixed with methanol showed a tan δ <1 with almost no dependence with frequency. This suggested that RSF without methanol behaved as a viscoelastic fluid (sol) while RSF with methanol showed characteristic solid (gel)-like behavior.[35] Secondly, the tan δ shifted from 0.83 to 0.04, at 1 Hz frequency, when methanol was changed from 5 to 37.5%; i.e. the tan δ steadily decreased with an increased quantity of methanol in the solution. And thirdly, G' increased from 0.36 to 4.6 × 10^3 Pa and similarly G'' increased from 0.30 to 0.18 × 10^3 Pa, at 1 Hz frequency, when methanol content was changed from 5 to 37.5%; i.e. both the moduli increased with an increased methanol content in the solution. The latter two observations collectively suggested that increasing amount of methanol in the solution led to increase in the extent of gel network formation and thereby an increase in the strength of the gel.[36]

3.6 Insights into RSF conformational changes from ATR-FTIR

To understand the non-solvent induced conformation changes in RSF, we performed the ATR-FTIR studies of the porous foams (freeze-dried hydrogels) prepared from RSF (2.5% w/v) mixed with variable amounts of methanol (5, 12.5, 25, 37.5 and 50% v/v, test). The freeze-dried RSF without methanol and the pure silk fibroin fiber were also analyzed for comparison purpose (controls). As presented in **Figure 7a**, the spectra of both the test and control samples showed absorption bands in the range of 1700-1600, 1600-1500 and 1200-1300 cm^{-1} that were characteristic of amide I (C=O stretching vibrations), II (C-N stretching and the N-H in-plane bending vibrations) and III (NH bending vibrations), respectively, of the silk fibroin.[37-39]

Further, there was neither appearance of new peaks nor complete suppression of existing signature peaks. It was thus clear that the addition of methanol does not affect the typical chemical composition of RSF. The detailed analysis of the amide I band revealed the changes in the chain conformation. As presented in **Figure 7b**, the control RSF showed a peak around 1635-1645 cm^{-1} that was typical of the less-ordered non-crystalline random coil component, while the control fiber showed a major peak between 1605-1635 cm^{-1} and a minor peak around 1697-1703 cm^{-1} that were characteristic of the ordered crystalline beta-sheet components.[21] While RSF mixed with 5% methanol exhibited peaks representative of both less-ordered and ordered structures. With further increasing methanol content, the test samples presented peaks typical of the ordered structure only. Therefore, it was clear that methanol induced the transformation of the random coil to beta-sheet transition in RSF, but there was a threshold amount of methanol that was needed to achieve the complete transformation.

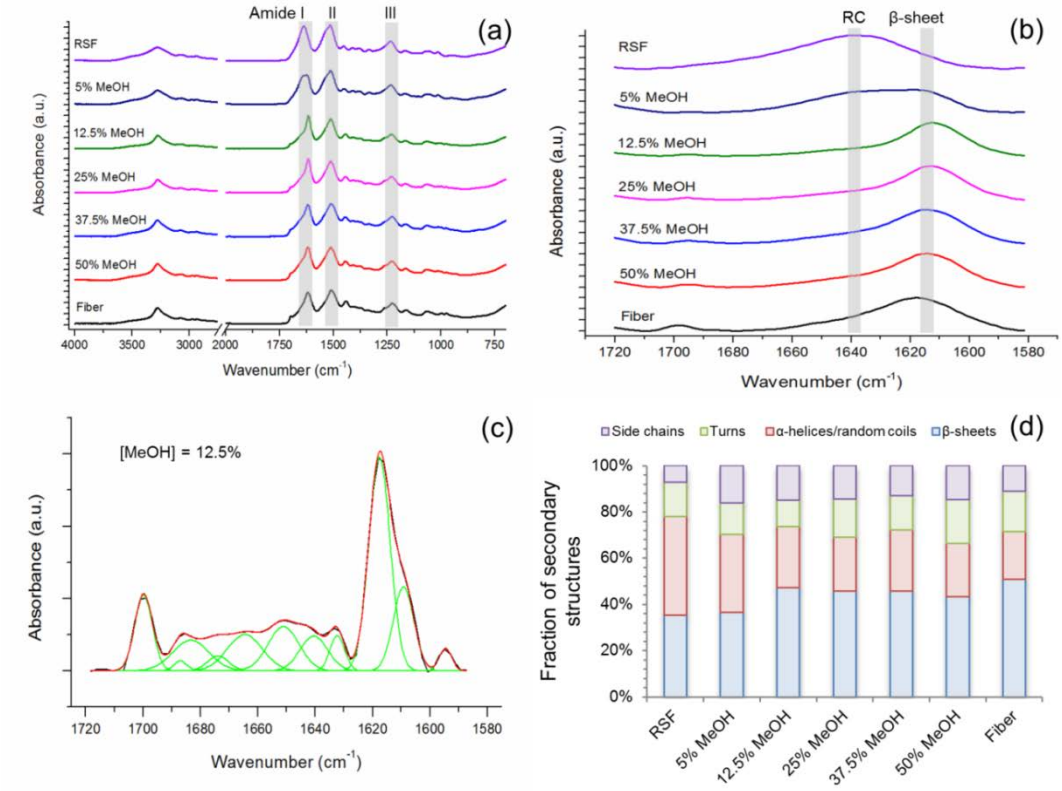

Figure 7. ATR-FTIR and Fourier self-deconvolution analysis: (a) the absorbance spectra of the freeze-dried hydrogels (porous foams) prepared from 2.5% w/v RSF mixed with variable amounts of methanol (MeOH) showed the characteristic amide I, II and II bands of RSF and suggested no changes in the chemical composition of RSF. (b) The amide-I region showed that the control RSF sample without methanol showed a peak at 1638-1655 cm^{-1} that was characteristic of random coil conformation of RSF, while, the control fiber sample showed a peak at 1605-1637 cm^{-1} that was typical of β-sheet conformation of RSF. Among the test samples, the one with 5% methanol showed peaks related to both states, while the ones with 12.5% or higher methanol showed peaks related to β-sheet conformation. (c) A representative FSD amide-I spectrum of RSF mixed with 12.5% methanol is shown here, the remaining spectra are enclosed in the supplementary information. (d) The FSD analysis revealed a decrease in the fraction of less-ordered secondary structural components and an increase in the fraction of ordered secondary structural components with an increase in methanol content.

To determine the fraction of individual secondary structure components, the amide I band was resolved by Fourier self-deconvolution analysis FSD. A typical deconvoluted amide I spectrum of RSF mixed with 12.5% methanol is presented in **Figure 7c**. The FSD spectra of the rest of the test and control samples are enclosed as supplementary figures (**Figure S2**-**S8**). The deconvoluted bands were assigned to the side chains, turns, α-helices, random coils or β-sheets by referring to the literature.[21-23] The sum of the individual secondary structural elements found in the control RSF, control fiber and test samples with variable amounts of methanol are illustrated in **Figure 7d**. The fraction of side chains as well as the fraction of turns remained nearly stable amongst all the test and control samples. However, the ratio of β-sheets to α-helices/random coils was 35 to 43% in the pure RSF and 51 to 21% in the pure fiber; the less-ordered nature of RSF and the ordered nature of the fiber were thus clearly evident. While the increase in methanol content reduced the α-helices/random coils components from 34 to 23% and increased the fraction of β-sheets from 36 to 47%. Further, when the fractions of less-ordered components (i.e. side chains, α-helices and random coils) and ordered components (turns and β-sheets) were summed and compared, the ratio of less-ordered to ordered elements changed from 50:50 to 62:38 with increased methanol content (**Figure S9**). These results were in a good agreement with those of Hu et al. 2006, who reported a similar decreasing trend in less-ordered components and increasing

trend in ordered components of RSF films post-treated with methanol for 1 to 4 days.[21]

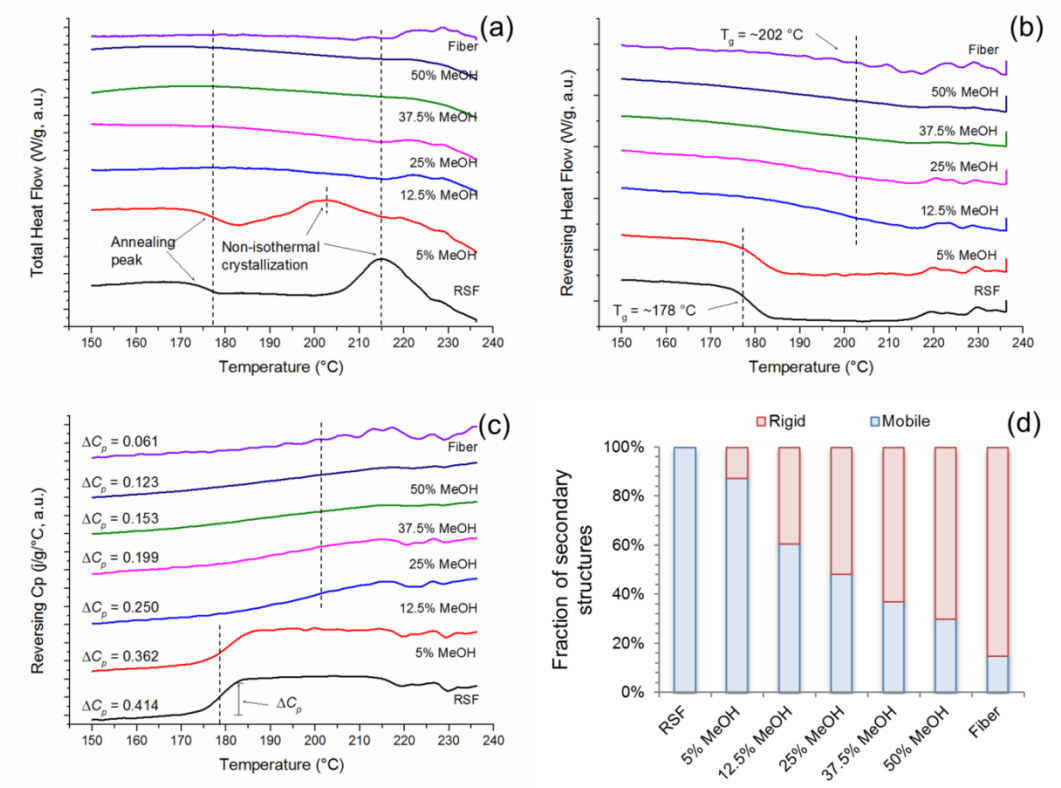

Figure 8. TM-DSC analysis: (a) The heat flow and (b) the reversing heat flow curves of the freeze-dried hydrogels (porous foams) prepared from 2.5% w/v RSF mixed with variable amounts of methanol (MeOH) showed the presence of a crystallization peak and a glass transition (Tg) peak at 178 °C in RSF mixed with 5% methanol, suggesting the presence of less-ordered structures similar to the control RSF; while, the rest of the samples showed a less prominent crystallization peak and a shift in Tg to 202 °C, suggesting the presence of ordered structures similar to the control fiber. (c) The specific reversing heat capacity and (d) the calculation of secondary structure composition revealed a decrease in the ΔC_p and an increase in the rigid elements with an increase in methanol content.

3.7 Insights into RSF phase transitions and crystallinity from TM-DSC

The TM-DSC offers excellent details on heat capacities, melting temperatures, crystallinity, etc., during the dynamic phase transitions of the macromolecules, which are otherwise not possible to obtain with the conventional heat-flux DSC.[21, 40] The TM-DSC results of the porous foams (freeze-dried hydrogels) prepared from RSF (2.5% w/v) mixed with a variable amount of methanol (5, 12.5, 25, 37.5 and 50% v/v, test) along with the freeze-dried RSF without methanol and the pure silk fibroin fiber (controls) are presented in **Figure 8**. As shown in **Figure 8a**, the total heat flow graph of the control RSF displayed a tiny downward signal at ~178 °C, a typical endothermic annealing peak representing the transition of RSF from the solid to liquid phase, and a prominent upward signal at ~213 °C, a typical exothermic peak representing the non-isothermal crystallization of RSF from the less-ordered to ordered state. The pure fibroin fiber exhibited a flat curve with no distinct endo or exothermic peaks which was attributed to its highly ordered crystalline structure with no/low scope for further phase transitions during the test scan range.[21, 41] On the other hand, RSF mixed with 5% methanol exhibited a similar endothermic peak as the control RSF, but the crystallization was less prominent and occurred at ~202 °C. The rest of the test samples showed no distinct endo or exothermic peaks similarly to the control fibroin fiber; the incline nature of the curves at ~202 °C was noticeable. It can be concluded that 5% of methanol in RSF solution induced the conformation transition but not sufficiently to achieve a complete crystallization and a higher methanol amount (i.e. 12.5% or more) increased the fraction of the crystallized content in RSF.

The reversing heat flow curves are presented in **Figure 8b**. The temperature of glass transition (T_g) of the control RSF and fibroin fibers were determined to be 178 and 202 °C, respectively. The T_g of RSF hydrogel made with 5% of methanol was 178 °C – similar to that of the control RSF; while T_g of RSF hydrogels made with 12.5% or higher methanol content was 202 °C – similar to that of the control fiber. Additionally, the change in the reversing heat capacity (ΔC_p) of the samples at their respective T_g were determined by following the literature.[21] The ΔC_p of RSF and fibers were 0.414 and 0.061 J/g/°C, respectively, whereas that of the test samples decreased from 0.362 to 0.123 J/g/°C with an increase in methanol content from 5 to 50 % (**Figure 8c**). Further, the ΔC_p was used to calculate the relative fraction of mobile and rigid structures following the equation 4; for this purpose, the control RSF was considered as 100% non-crystalline structure and its heat capacity was taken as ΔC_p^{nc}. As displayed in **Figure 8d**, with respect to the control RSF, the ratio of mobile to rigid

structural elements in the control fibroin fiber was 0.15:0.85, while in the test samples it changed from 0.87:0.13 to 0.30:0.70 with increasing methanol content. Therefore, it can be concluded that the addition of methanol induced the structural transitions in RSF from less-ordered to rigid structures (β-sheets and/or highly-constrained non-crystalline immobile elements such as β-turns); such an increase in the rigid elements a) restricted the relaxation of mobile elements and thus elevated the T_g from 178 to 202 ^{o}C, and b) reduced the mass fraction of mobile elements and thus decreased the ΔC_p from 0.414 to 0.123 J/g/ ^{o}C.[21, 41]

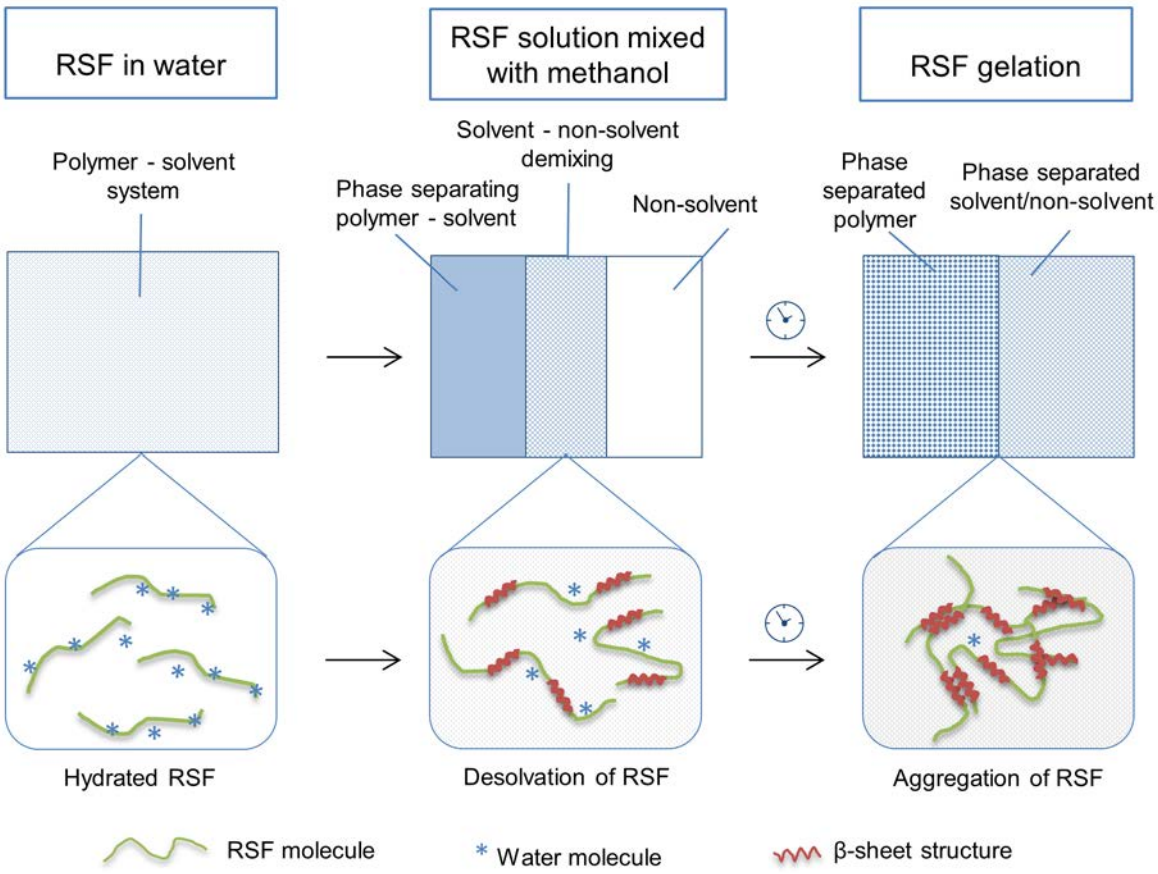

Figure 9. Mechanism of RSF hydrogels by non-solvent induced phase separation: In the aqueous state, the water molecules stabilize RSF molecules by decreasing its inter- and intra-molecular friction and thereby expanding the accessible conformational space. However, when a non-solvent such as methanol was added, RSF – water – methanol system behaves as the polymer – solvent – non-solvent ternary system wherein methanol participates in a proton exchange with water and thus disturbs the interactions between water and RSF. This causes the desolvation of RSF; and, the meta-stable hydrophobic and block copolymer nature of RSF prompts the conformational transformations that eventually lead to the phase separation or aggregation of RSF with a highly ordered crystalline structure.

3.8 Possible gelation mechanism

B. mori silk fibroin is a large bio-macromolecule consisting of a heavy chain (~350 kDa) and a light chain (25 kDa). The determination of fibroin molecular sequence has established it as a natural repetitive block copolymer with highly-hydrophobic crystalline domains consisting of short side chain amino acids interspersed in less-hydrophobic amorphous domains consisting of bulkier side chain amino acids.[1, 42] This block copolymer nature of the fibroin gives it the intrinsic propensity to transform the silk-I structure (a water-soluble and meta-stable form of fibroin existing in the silkworm silk gland) to a silk-II structure (a water-insoluble and highly stable form of fibroin formed when the silkworm starts spinning the fiber), which is characterized by a β-sheet secondary structure stabilized by inter-chain hydrogen bonds and inter-sheet hydrophobic interactions.[1, 42] In the native state, such transformation occurs via the shear forces exerted at the spinneret, along with other defined/undefined forces.[43, 44] In the current study, we exploited the meta-stable nature of reconstituted silk fibroin (RSF) which was similar to silk-I structure of native fibroin and its sensitivity towards the organic solvents to induce the conformational changes that eventually led to the self-assembly and the formation of a hydrogel.

In order to understand how methanol induced the aggregation of RSF, we turned to the basic concept of solubility. The role of a solvent (i.e. water in case of biopolymers) in the assembly, phase transition and structural stability of a protein is well-studied.[9, 45, 46] The stability of a protein polymer is attributed to the interactions of the water molecules with its specific functional groups via hydrogen bonding, van der Waals or hydrophobic interactions that

expand its accessible conformational space by decreasing the inter- and intra-molecular friction. However, when the polymer is prone to desolvation, the polymer returns to its thermodynamically stable glassy state. The same desolvation phenomenon was held responsible in the native state silk fiber formation.[47, 48] In this perspective, the fibroin – water – polar protic organic solvent system in the current study can be regarded as a polymer – solvent – non-solvent ternary system wherein the organic solvent participates in the proton exchange with the water and thus disturbs the interactions between water and RSF molecule. This causes the desolvation of RSF; and eventually, the meta-stable and block copolymer nature of RSF prompts its transformation from a less-ordered amorphous form (similar to native silk-I form) to a highly-ordered crystalline form (similar to native silk-II form) (**Figure 9**). Our conclusion complies with a recent study by Numata et al., 2011 on the silk fibroin gelation in presence of ethanol.[49]

Although we do not present any data on molecular interactions in the fibroin – water – methanol system, we do submit data that confirms the non-solvent induced phase separation of RSF solution that led to gelation. For example, we found that the freeze-dried RSF was readily water-soluble due to lack of rigid secondary structure when compared with the freeze-dried RSF hydrogel which was water-insoluble. As evident from rheometry results, the tan δ of the pure RSF was >1 that represents its sol-like behavior, while RSF mixed with methanol exhibits gel-like behavior with tan δ <1. The FTIR studies and subsequent FSD analysis revealed that the content of less-ordered secondary structural elements was higher in the pure RSF, whereas the content of high-ordered elements was higher in RSF hydrogels. And, as evident from TM-DSC, the pure RSF showed presence of thermally induced crystallization and high specific heat capacity increment in comparison with RSF hydrogel which showed reduced specific heat increment with no thermally induced crystallization. Further, the gradual increase in the rigidity of RSF chains with increasing methanol content suggested the dose dependent behavior of the system. Our observations of non-solvent induced transformation of RSF conformations are in good agreement with those induced by changing pH,[10] applying electric field,[32] ultra-sonication,[41] shear,[50] or by blending with hydroxypropylcellulose,[33] Poly(N-isopropylacrylamide).[34]

Conclusions‡

Although the effects of the organic solvents such as methanol on RSF have long been known, here we present a fresh perspective on their interactions that in our experiments resulted in RSF aggregation or gelation by the phenomenon of non-solvent induced phase separation (NIPS). We showed that the addition of 12.5% v/v methanol induced the gelation of 2.5% w/v RSF in 10 h at 22 °C temperature. The porous foams were obtained after lyophilization of the hydrogels and were found to have porosity of 88%, water holding capacity of 99% and swelling index of 8.6. The rheological studies revealed the typical kinetics of RSF gelation with a crossover of storage and loss modulus curves at 8.7 h, and a gradual decrease in tan δ with increasing methanol content. The ATR-FTIR and FSD analysis of amide I revealed a decrease in the less-ordered and an increase in the ordered secondary structural elements of RSF with an increase in methanol volume. Additionally, the TM-DSC data showed a shift in T_g and more importantly an increase in the content of rigid structures of RSF with an increase in the amount of methanol. Taken together, it was evident that RSF – water – protic organic solvent mixture behaved as a polymer – solvent – non-solvent ternary phase system, wherein the demixing of the water – protic organic solvent phases altered the thermodynamic equilibrium of RSF – water phases and resulted in the desolvation and eventual separation of RSF phase. The gelation time as well as the properties of hydrogels and porous foams can be controlled by the amount of non-solvent, by RSF concentration and by incubation temperature. Further, RSF gelation was achieved by a range of protic organic solvents such as methanol, ethanol, isopropanol and n-butanol but not by aprotic organic solvents such as dimethyl sulfoxide at least during an overnight incubation at room temperature. The NIPS induced RSF gelation may be further exploited for the encapsulation of cells and/or for the controlled release of hydrophilic and hydrophobic drugs.

Acknowledgements

Authors thank the funding received from the Ministry of Education, Youth and Sports, Czech Republic (EE2.3.30.0029 to DK), the European Regional Development Fund, Czech Republic (CZ.1.05/1.1.00/02.0109 to DK), the Air Force Office of Scientific Research (FA9550-12-1-0294 to FV) and the European Research Council (SP2-GA-2008-233409 to FV). NK thanks FV for the kind invitation to visit his Oxford Silk Group lab, and Dr. Darshil Shah (a colleague at the OSG, Oxford) and Dr. Marta Kumorek (a colleague at the IMC, Prague) for helpful discussions.

Notes and references

‡It must be noted that the morphological, physical and structural properties data and the conclusions thereof showed in this study were representative of the porous foams i.e. the freeze-dried form of the hydrogel. They may or may not represent the wet form of the hydrogel in its absolute sense, yet the relative differences in a given series may be comparable.

1. K. Tanaka, N. Kajiyama, K. Ishikura, S. Waga, A. Kikuchi, K. Ohtomo, T. Takagi and S. Mizuno, *BBA-Protein Struct. M.*, 1999, **1432**, 92-103.
2. M. N. Padamwar and A. P. Pawar, *J. Sci. Ind. Res.*, 2004, **63**, 323-329.
3. N. Kasoju and U. Bora, *Adv. Healthcare Mater.*, 2012, **1**, 393-412.
4. C. Vepari and D. L. Kaplan, *Prog Polym Sci*, 2007, **32**, 991-1007.
5. D. N. Rockwood, R. C. Preda, T. Yucel, X. Wang, M. L. Lovett and D. L. Kaplan, *Nat. Protoc.*, 2011, **6**, 1612-1631.

6. N. Kasoju and U. Bora, *Biomed. Mater.*, 2012, **7**, 045004.
7. J. L. Drury and D. J. Mooney, *Biomaterials*, 2003, **24**, 4337-4351.
8. F. N. Braun and C. Viney, *Int. J. Biol. Macromol.*, 2003, **32**, 59-65.
9. C. Dicko, N. Kasoju, N. Hawkins and F. Vollrath, *Soft Matter*, 2015, DOI: 10.1039/C5SM02036K.
10. A. E. Terry, D. P. Knight, D. Porter and F. Vollrath, *Biomacromolecules*, 2004, **5**, 768-772.
11. R. R. Mallepally, M. A. Marin and M. A. McHugh, *Acta Biomater.*, 2014, **10**, 4419-4424.
12. T. Yucel, P. Cebe and D. L. Kaplan, *Biophys. J.*, 2009, **97**, 2044-2050.
13. X. Wang, J. A. Kluge, G. G. Leisk and D. L. Kaplan, *Biomaterials*, 2008, **29**, 1054-1064.
14. N. Guziewicz, A. Best, B. Perez-Ramirez and D. L. Kaplan, *Biomaterials*, 2011, **32**, 2642-2650.
15. Y. Luyuan, Y. Mohammed, Z. Xiubo, C. Paul, P. Fang, W. Yuming, X. Hai, W. John and R. L. Jian, *Biomed. Mater.*, 2015, **10**, 025003.
16. M. Tsukada, G. Freddi, N. Minoura and G. Allara, *J. Appl. Polym. Sci.*, 1994, **54**, 507-514.
17. J. Nam and Y. H. Park, *J. Appl. Polym. Sci.*, 2001, **81**, 3008-3021.
18. R. Nazarov, H.-J. Jin and D. L. Kaplan, *Biomacromolecules*, 2004, **5**, 718-726.
19. T. Debnath, S. Ghosh, U. S. Potlapuvu, L. Kona, S. R. Kamaraju, S. Sarkar, S. Gaddam and L. K. Chelluri, *PloS one*, 2015, **10**, e0120803.
20. B. Sarker, R. Singh, R. Silva, J. A. Roether, J. Kaschta, R. Detsch, D. W. Schubert, I. Cicha and A. R. Boccaccini, *PloS one*, 2014, **9**, e107952.
21. X. Hu, D. L. Kaplan and P. Cebe, *Macromolecules*, 2006, **39**, 6161–6170.
22. A. Dong, J. Matsuura, S. D. Allison, E. Chrisman, M. C. Manning and J. F. Carpenter, *Biochemistry*, 1996, **35**, 1450-1457.
23. A. Dong, B. Caughey, W. S. Caughey, K. S. Bhat and J. E. Coe, *Biochemistry*, 1992, **31**, 9364-9370.
24. P. Shi, S. A. Abbah, K. Saran, Y. Zhang, J. Li, H.-K. Wong and J. C. H. Goh, *Biomacromolecules*, 2013, **14**, 4465-4474.
25. B. Du, J. Wang, Z. Zhou, H. Tang, X. Li, Y. Liu and Q. Zhang, *Chem. Commun.*, 2014, **50**, 4423-4426.
26. Y. Tamada, *Biomacromolecules*, 2005, **6**, 3100-3106.
27. U.-J. Kim, J. Park, C. Li, H.-J. Jin, R. Valluzzi and D. L. Kaplan, *Biomacromolecules*, 2004, **5**, 786-792.
28. N. Kasoju, D. Kubies, M. M. Kumorek, J. Kriz, E. Fabryova, L. Machova, J. Kovarova and F. Rypacek, *PloS one*, 2014, **9**, e108792.
29. S. Nagarkar, T. Nicolai, C. Chassenieux and A. Lele, *Phys. Chem. Chem. Phys.*, 2010, **12**, 3834-3844.
30. S. Backlund, H. Høiland and I. Vikholm, *J. Solution Chem.*, 1984, **13**, 749-755.
31. N. Kasoju and U. Bora, *J. Biomed. Mater. Res. Part B Appl. Biomater.*, 2012, **100**, 1854-1866.
32. T. Yucel, N. Kojic, G. G. Leisk, T. J. Lo and D. L. Kaplan, *J. Struct. Biol.*, 2010, **170**, 406-412.
33. Z. Gong, Y. Yang, Q. Ren, X. Chen and Z. Shao, *Soft Matter*, 2012, **8**, 2875-2883.
34. T. Wang, L.-l. Zhang and X.-j. He, *J. Nanomater.*, 2013, **2013**, 9.
35. M. Boulet-Audet, A. E. Terry, F. Vollrath and C. Holland, *Acta Biomater.*, 2014, **10**, 776-784.
36. B. B. Mandal, S. Kapoor and S. C. Kundu, *Biomaterials*, 2009, **30**, 2826-2836.
37. J. Shao, J. Zheng, J. Liu and C. M. Carr, *J. Appl. Polym. Sci.*, 2005, **96**, 1999-2004.
38. H. Zhang, L.-l. Li, F.-y. Dai, H.-h. Zhang, B. Ni, W. Zhou, X. Yang and Y.-z. Wu, *J. Transl. Med.*, 2012, **10**, 1-9.
39. V. M. Swinerd, A. M. Collins, N. J. V. Skaer, T. Gheysens and S. Mann, *Soft Matter*, 2007, **3**, 1377-1380.
40. M. Reading, D. Elliott and V. L. Hill, *J. Therm. Anal.*, 1993, **40**, 949-955.
41. X. Hu, Q. Lu, L. Sun, P. Cebe, X. Wang, X. Zhang and D. L. Kaplan, *Biomacromolecules*, 2010, **11**, 3178-3188.
42. D. L. Kaplan, S. Fossey, C. M. Mello, S. Arcidiacono, K. Senecal, W. Muller, S. Stockwell, R. Beckwitt, C. Viney and K. Kerkam, *MRS Bull.*, 1992, **17**, 41-47.
43. F. Vollrath, D. Porter and C. Holland, *MRS Bull.*, 2013, **38**, 73-80.
44. C. Holland, J. S. Urbach and D. L. Blair, *Soft Matter*, 2012, **8**, 2590-2594.
45. D. Porter and F. Vollrath, *Soft Matter*, 2013, **9**, 643-646.
46. D. Porter and F. Vollrath, *BBA Proteins Proteom.*, 2012, **1824**, 785-791.
47. D. Porter and F. Vollrath, *Soft Matter*, 2008, **4**, 328-336.
48. A. Matsumoto, J. Chen, A. L. Collette, U.-J. Kim, G. H. Altman, P. Cebe and D. L. Kaplan, *J. Phys. Chem. B*, 2006, **110**, 21630-21638.
49. K. Numata, T. Katashima and T. Sakai, *Biomacromolecules*, 2011, **12**, 2137-2144.
50. I. Greving, M. Cai, F. Vollrath and H. C. Schniepp, *Biomacromolecules*, 2012, **13**, 676-682.

Kasoju et al., Silk Fibroin Gelation via Non-Solvent Induced Phase Separation, 2015
(Manuscript ID: BM-ART-10-2015-000471.R1)

Graphical TOC

The metastable nature of reconstituted silk fibroin (RSF) and its sensitivity to the solvent quality were explored to make hydrogels and porous foams that could be useful for the encapsulation of cells and/or hydrophilic and hydrophobic drugs.